Selective Insertion of La-Oxides into Micropores of SBA-15 and Preparation of highly Ordered Mesoporous La-Si Oxides with High Stability against Alkaline Hydrolysis

Yoshimi Kawamoto,[1] Jinri Li,[1] Yusuke Ide,[2] Tsuneji Sano,[1] and Masahiro Sadakane*[1]

[1]Applied Chemistry Program, Graduate School of Advanced Science and Engineering, Hiroshima University, 1-4-1 Kagamiyama, Higashi-Hiroshima 739-8527, Japan.
[2]Research Center for Materials Nanoarchitectronics (MANA) National Institute for Materials Science (NIMS), 1-1 Namiki, Tsukuba, Ibaraki, 305-0044, Japan.

*Corresponding author: *Hiroshima University, 1-4-1 Kagamiyama, Higashi-Hiroshima 739-8527,* Email: sadakane09@hiroshima-u.ac.jp

Abstract

Lanthanum oxides were selectively inserted into the micropores of SBA-15 via a simple impregnation and subsequent calcination method, forming mesoporous La-Si oxides (SBA-La). Characterization by XRD, N_2 adsorption, and TEM confirmed that La oxides preferentially fill the micropores without damaging the mesopore structure. Upon excess loading, La oxides occupy mesopores while retaining cylindrical mesoporous morphology. SBA-La exhibits significantly enhanced stability against alkaline hydrothermal conditions compared to unmodified SBA-15. The improved durability is attributed to the formation of La oxides in micropores, which suppresses degradation pathways. This strategy provides a simple and effective route to improve the chemical robustness of mesoporous silica materials.

Keywords: SBA-15, mesoporous La-Si oxide, High stability

Graphical abstract

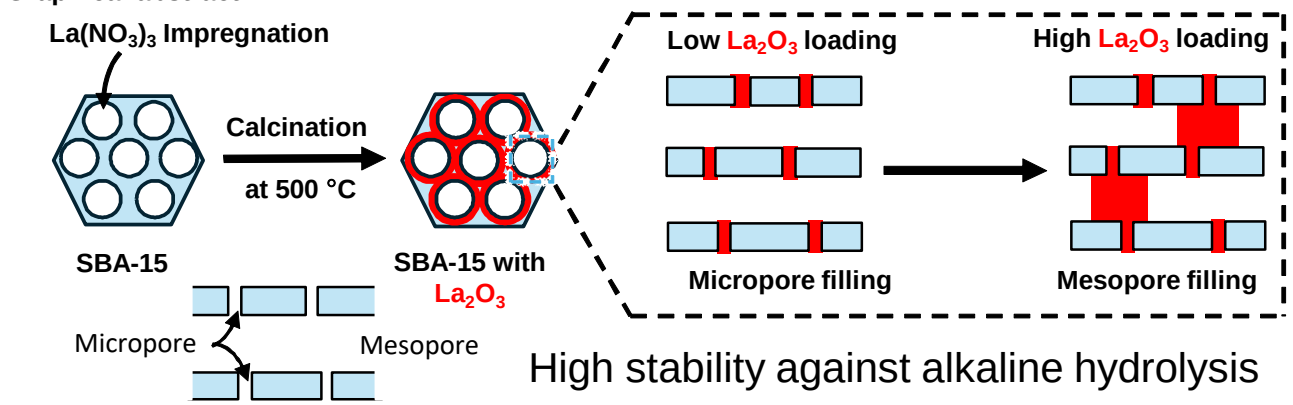

Mesoporous silica with well-ordered pores (pore diameters of 2 – 50 nm) have attracted considerable attention, because these materials have large surface area and their pore sizes are large enough to entrap large organic molecules which do not enter in microporous materials such as zeolites. Therefore, they have been utilized or investigated in variety of field such as catalysis,[1, 2] separation,[3] drug delivery,[4] and CO_2 adsorption materials.[5] One serious disadvantage of mesoporous silica materials is instability under alkaline hydrolysis condition.[6]

Among the various mesoporous silicas, SBA-15 with hexagonally ordered mesopore channel connected by micropores (Scheme S1) have attracted great interest due to their larger pores, tunability of pore size, thicker pore walls, and significant amounts of micropores in the walls.[2] Due to the thick walls, SBA-15 has higher stability than other mesoporous silicas, however, further improvement of stability is needed.

It is known that there is strong interaction between lanthanoid metal with silicas. Rodriguez-Izquierdo group reported that calcination of $La(NO_3)_3$ with silica (Cabosil M-5) produced La-silicate.[7] Schüth group reported that lanthanum oxides coat the surface of mesopores of SBA-15 due to strong interaction between the lanthanoid metal and silica.[8] Xue group also reported $La(NO_3)_3$ is a suitable reagent to coat the surface of mesopores with lanthanum oxide,[9] and Fang group reported that lanthanum reacted with silanol moiety.[10]

In this study, we present that lanthanum oxide selectively inserts into the micropores of SBA-15 by a simple impregnation-calcination method. By filling micropores of SBA-15 with La oxides, well-ordered mesoporous La-Si oxides (SBA-La) are produced. When

the volume of La oxide exceeds the micropore volume, La oxide begins to occupy the mesopores. These SBA-La show high stability against alkaline hydrolysis, whereas parent SBA-15 collapses.

$La(NO_3)_3$-$6H_2O$ was impregnated in SBA-15 by stirring SBA-15 in ethanol solution of $La(NO_3)_3$-$6H_2O$ at room temperature until the solvent was evaporated. They were calcined in a muffle oven in air at 500 ºC for 3 hours. TG-DTA curves of SBA-15-$La(NO_3)_3$ composite before the calcination, indicated that calcination at 500 ºC is enough to decompose $La(NO_3)_3$ (Fig. S1), which was also confirmed by the decrease of a IR band at ca. 1385 cm^{-1} for NO_3^- (Fig. S2 (f)). The prepared samples were denoted as SBA-La(X), where X represented amount (mmol) of $La(NO_3)_3$ with 1g of SBA-15.

Small angle XRD pattern of SBA-15 used in this work exhibited the three characteristic peaks of the (100), (110), and (200) lattice planes of the hexagonal (P6mm) pore structure (Fig. 1(a)). Nitrogen adsorption-desorption isotherm of the SBA-15 revealed type IV behavior typical for mesoporous materials with type H1 hysteresis loop (adsorption and desorption branches are parallel) (Fig. 2 (a) and Table S1). The type H1 hysteresis is characteristic for cylindrical pores.[11] IR spectra exhibits bands at 1095 and 807 cm^{-1} correspond to the vibrations of Si-O-Si, and 965 cm^{-1} correspond to the vibrations of Si-O of silanol (Fig. S2 (b)).[10]

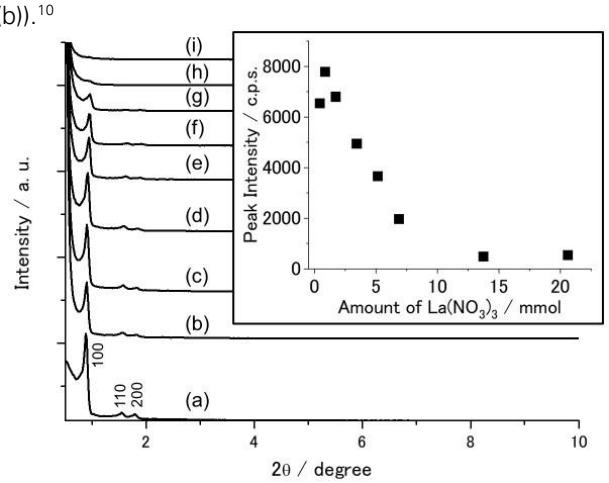

Fig. 1. XRD patterns of (a) SBA-15 and SBA-La(X) prepared using (b) 0.43, (c) 0.86, (d) 1.72, (e) 3.44, (f) 5.16, (g) 6.87, (h) 13.75, and (i) 20.62 mmol of $La(NO_3)_3$. (inset) Peak intensities of 100 peak against amount of $La(NO_3)_3$.

Three XRD peaks characteristic for hexagonal porous structure remained until SBA-15-La(6.87) (Fig. 1(g)) indicating presence of mesopores. Wide angle XRD did not show any distinct peaks (Fig. S3 (d)), indicating the obtained compound consists of both amorphous silica and amorphous Lanthanum species.

Morphologies of SBA-La were similar to the SBA-15 and no plate-like particle of La oxide was observed even in the SBA-15-La(20.62) (Fig. S4), indicating all the La oxides exist in the pores of SBA-15.

The obtained solids were analyzed using nitrogen adsorption-desorption isotherm (Fig. 2). The type IV isotherms were obtained until SBA-15-La(6.87) (Fig. 2(g)) suggesting presence of mesopores similar to XRD results. Obtained porous properties were summarized in Table S1 and the estimated microporous volumes and mesoporous volumes per 1g of SBA-15, respectively, were plotted against amount of $La(NO_3)_3$ (Fig. 3). Addition of a small amount (until 1.72 mmol) of $La(NO_3)_3$ decreased adsorbed N_2 at very low P/P_0 corresponding to the micropore volumes whereas amount of uptake at P/P_0 of ca. 0.7 corresponds to the mesopore volumes kept almost constant (Table S1 and Fig. 3). This result indicates that La oxides selectively filled into the micropores until all micropores are filled with La oxides. The amount of 1.72 mmol is smaller but in the same range to the calculated value of 4.0 mmol assuming that the micropore (volume: 0.10 $cm^3\ g^{-1}$) was filled with crystalline La_2O_3 (MW: 325.81 g mol^{-1}; density: 6.51 g cm^{-3}). We believe that this difference is due to amorphous nature of La oxide in the micropore.

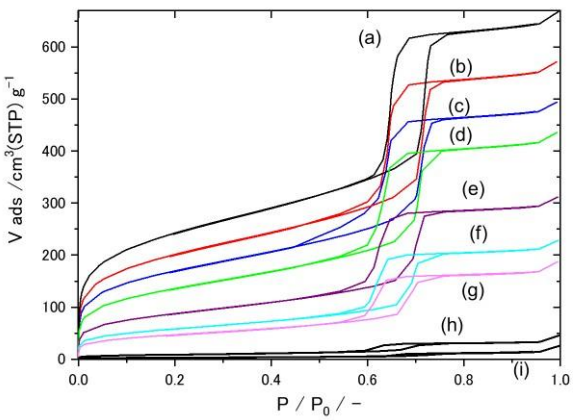

Fig. 2. Nitrogen adsorption-desorption isotherms of (a) SBA-15 and SBA-La(X) prepared using (b) 0.43, (c) 0.86, (d) 1.72, (e) 3.44, (f) 5.16, (g) 6.87, (h) 13.75, and (i) 20.62 mmol of $La(NO_3)_3$.

Interestingly, sharp H1-type hysteresis loops were retained even if large amount of $La(NO_3)_3$ was loaded, indicating that cylinder-shape mesopores was maintained. It is reported that the hysteresis loop was affected by loading of metal oxides in the mesopore. If the mesopores were homogeneously coated by metal oxide, H1-type hysteresis was observed with decreased mesopore diameter.[12] If the metal oxide particles were attached on the mesopore walls, desorption branch of hysteresis became stepwise.[13] In our case, the relative pressure of adsorption branch of hysteresis and therefore BJH mesopore diameter do not change until large amount of La oxides was loaded (Fig. 2). After the micropores are filled, La oxides fill the mesopores without changing mesopore diameters (Scheme S1). The selective insertion of $La(NO_3)_3$ was

also confirmed by powder XRD. Until 1.72 mmol, the intensities of characteristic peak for hexagonal walls did not decrease, but the peak intensity gradually decreased when mesopore was filled by La oxides (Fig. 1, inset). Filling of mesopores decreased X-ray scattering difference between the hexagonal wall and mesopores.

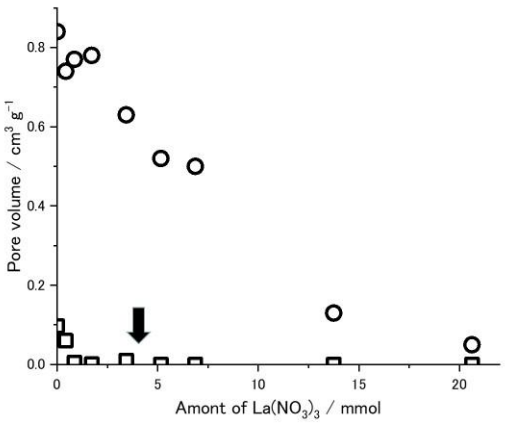

Fig. 3. (open circles) mesopore volumes and (open squares) micropore volumes per 1.0 g of SBA-15 against amount of $La(NO_3)_3$. An arrow indicates amount (4.0 mmol) of $La(NO_3)_3$ to fill only micropore of SBA-15 (1.0 g) with La_2O_3 crystal.

Filling of La oxide in the mesopores were also confirmed by TEM. Channel-like pores were observed until the micropores were filled, but pore and wall contrast became small when mesopores were started to be filled (Fig. S5).

In order to ensure this filling model, we have performed IR measurement (Fig. S2 (c)), where IR peak corresponding to Si-OH at 965 cm^{-1} disappeared by filling of micropores by La loading. SBA-15 was prepared using a block copolymer of poly(ethylene oxide) and poly(propylene oxide) as a template, and micropores were formed around hydrophilic polyethylene oxide moiety. Therefore, it is expected that large amount of Si-OH group exists in the micropores.[14-16] Disappearance of Si-OH group agrees with our model where micropore is first filled by La oxides.[9, 10]

To understand transformation behavior of $La(NO_3)_3$ in SBA-15, SBA-15-$La(NO_3)_3$(6.87) heated at different temperatures were characterized by powder XRD (Fig. S6) and N_2 isotherm (Fig. S7). We selected sample with 6.87 mmol of $La(NO_3)_3$ because the estimated volume of 1.29 cm^3 with density of 2.3 g cm^{-3} is larger than sum of micropore and mesopore volume of SBA-15. Characteristic powder XRD pattern for SBA-15 was not observed until the sample was heated at 200 ºC, but started to appear when heating temperature was more than 300 ºC (Fig. S6), indicating that the mesopores were filled with mixture of La nitrate, La oxide and La hydroxide (La-oxo-nitrate) at temperatures until at 300 ºC and the mesopores were opened at 400 ºC. This phenomenon was also confirmed by N_2 isotherm. Adsorption uptake into mesopores at ca. 0.6-0.7 of P/P_0 gradually increased and the desorption at ca. 0.7-0.4 of P/P_0 occurred stepwise after heating at 200 and 300 ºC indicating presence of La-oxo-nitrate particles in the mesopores (Scheme S2). Adsorption and desorption became sharp and H1-type hysteresis loops was obtained after heating at 400 ºC. The characteristic powder XRD pattern and the sharp H1-type hysteresis was kept after heating at 800 ºC. Further heating decomposed mesoporous structure.

We also checked the possibility of insertion of Co, Fe, and Ce oxides under same conditions in the SBA-15. N_2 isotherms and XRD pattern with different metal amount were shown in Fig. S8, and micropore volumes and mesopore volumes after calcination at 500 ºC were summarized in Fig. S9. In the cases of Fe, Co, and Ce, micropores were still open when enough metal was impregnated to fill the micropores indicative of non-selective insertion into the micropores.

Enhancement of stability against alkaline hydrolysis is one of the most important modifications of SBA-15 related materials, and doping of Al has been reported to be effective. We checked hydrolysis stability by heating samples at 60 ºC in the 2M NaOH solution for 2 hours where bare SBA-15 dissolved completely and SBA-15 hard template dissolved from SBA-15-metal oxide composites (Metal: Co, Fe, Ce, Ni, etc).[6, 17] The SBA-La samples, on the other hand, did not dissolve under the NaOH treatments, and the remained amount and the mesopore volumes were summarized in Table S2. As confirmed by XRD (Fig. S10 (a)-(b)), only some SBA-La samples retained mesoporous structure. The remaining amount increased by increasing La loading amount, indicated that La enhances the stability against alkaline hydrolysis. When loading of La was higher than 3.44 mmol/g-SBA, in which micropore were fully filled with La oxide, the XRD peaks corresponding to the mesopore was kept after NaOH treatment (Fig. S10(b)). When the amount of La was lower than 3.44 mmol/g-SBA, the characteristic XRD peaks disappeared. Well-defined H1-type hysteresis loop was obtained in the case of SBA-La(5.16) and SBA-La(6.87) (Fig. S10(c)) where XRD peaks were observed. These results indicate that micropore filling of La increased stabilities against alkaline hydrolysis. TEM images of samples after NaOH treatment clearly indicated that SBA-La(1.72) contained less ordered mesopore whereas SBA-La(5.16) retained well-ordered mesopores (Fig. 4).

We also checked stability by heating the samples in the presence of NH_3 and H_2O vapor (Fig. S11). As shown in Fig. S12, XRD pattern of SBA-15 and SBA-La(1.72) disappeared after hydration treatment for 3 hours, whereas one of SBA-15-La (5.16) remained after 7 day. N_2 isotherm indicated that mesopores of SBA-15 was decomposed after 3 hours NH_3 hydrothermal treatment, although one of SBA-La(5.16) remained after 7 days (Fig. 5 and S12). On the other hand, SBA-M(5.16) (M = Co, Fe, and Ce), did not kept the

mesoporous structure after 3 hours treatment. It is reported that degradation of SBA-15 starts in the micropores where reactive Si-OH is present.[18] Filling of the micropore enhanced hydrolysis stability.

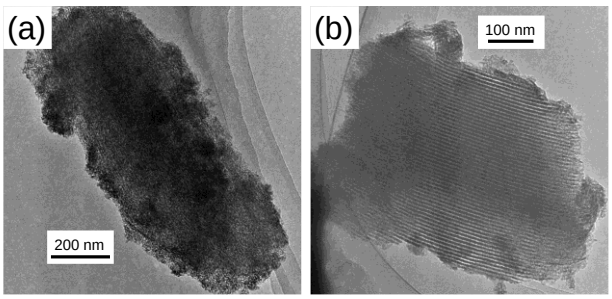

Fig. 4 TEM images of (a) SBA-La(1.72) and (b) SBA-La(5.16) after NaOH treatments.

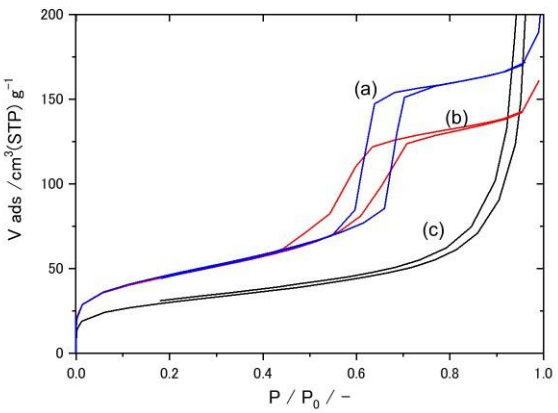

Fig. 5 Nitrogen adsorption-desorption isotherms of SBA-La(5.16) (a) before and (b) after NH_3 hydrothermal treatment (3 hours), and (c) SBA-15 after NH_3 hydrothermal treatment (3 hours).

Selective insertion of lanthanum oxides into SBA-15 micropores produced mesoporous La-Si oxides with preserved structure and significantly enhanced stability. The micropore filling suppressed degradation under alkaline and hydrothermal conditions. This simple strategy provides an effective route to improve the durability of mesoporous silica materials for advanced catalytic and adsorption applications.

Supplementary data

Supplementary material is available at *Chemistry Letters*

Funding

This work was supported by SUZUKI foundation, JSPS KAKENHI Grant-in-Aid for transformative Research Area (A) "Supra-ceramics" (JP22H05144), and JSPS Core-to-Core Program.

Conflict of interest statement. None declared.

References

1 A. Velty, A. Corma, *Chem. Soc. Rev.* **2023**, *52*, 1773, http://doi.org/10.1039/d2cs00456a.
2 P. Verma, Y. Kuwahara, K. Mori, R. Raja, H. Yamashita, *Nanoscale* **2020**, *12*, 11333, http://doi.org/10.1039/d0nr00732c.
3 E. Da'na, *Microporous Mesoporous Mater.* **2017**, *247*, 145, http://doi.org/10.1016/j.micromeso.2017.03.050.
4 V. F. Vavsari, G. M. Ziarani, A. Badieic, *RSC Adv.* **2015**, *5*, 91686, http://doi.org/10.1039/c5ra17780d.
5 J. Li, N. Tsunoji, R. Kumar, N. C. Sukmana, M. Sadakane, *J. Porous Mater.* **2024**, *31*, 1289, http://doi.org/10.1007/s10934-024-01596-7.
6 X. Deng, K. Chen, H. Tüysüz, *Chem. Mater.* **2017**, *29*, 40, http://doi.org/10.1021/acs.chemmater.6b02645.
7 H. Vidal, S. Bernal, R. T. Baker, D. Finol, J. A. P. Omil, J. M. Pintado, J. M. Rodríguez-Izquierdo, *J. Catal.* **1999**, *183*, 53.
8 J. Sauer, F. Marlow, B. Spliethoff, F. Schüth, *Chem. Mater.* **2002**, *14*, 217.
9 X. Sheng, Y. Zhou, Y. Duan, Y. Zhang, M. Xue, *J. Porous Mater.* **2011**, *18*, 677, http://doi.org/10.1007/s10934-010-9426-9.
10 X. Miao, W. Shen, X. Gao, Y. Fang, *J. Porous Mater.* **2021**, *28*, 1493, http://doi.org/10.1007/s10934-021-01100-5.
11 K. S. W. Sing, D. H. Everett, R. A. W. Haul, L. Moscou, R. A. Pierotti, J. Rouquerol, T. Siemieniewska, *Pure Appl. Chem* **1985**, *57*, 603.
12 Y. J. Pagán-Torres, J. M. R. Gallo, D. Wang, H. N. Pham, J. A. Libera, C. L. Marshall, J. W. Elam, A. K. Datye, J. A. Dumesic, *ACS Catal.* **2011**, *1*, 1234, http://doi.org/10.1021/cs200367t.
13 P. V. D. Voort, P. I. Ravikovitch, K. P. D. Jong, M. Benjelloun, E. V. Bavel, A. H. Janssen, A. V. Neimark, B. M. Weckhuysen, E. F. Vansant, *J. Phys. Chem. B* **2002**, *106*, 5873, http://doi.org/10.1021/jp025642i.
14 K. Sugino, N. Oya, N. Yoshie, M. Ogura, *J. Am. Chem. Soc.* **2011**, *133*, 20030, http://doi.org/10.1021/ja2070522.
15 S. Maaz, M. Rose, R. Palkovits, *Microporous Mesoporous Mater.* **2016**, *220*, 183, http://doi.org/10.1016/j.micromeso.2015.09.005.
16 A. Centineo, H. G. T. Nguyen, L. Espinal, J. C. Horn, S. Brandani, *Microporous Mesoporous Mater* **2019**, *282*, http://doi.org/10.1016/j.micromeso.2019.03.018.
17 S. Guptaa, C. Ciotonea, S. Royer, J.-P. Dacquin, C. P. Vinod, *Appl. Mater. Today* **2020**, *19*, 100586, http://doi.org/10.1016/j.apmt.2020.100586.
18 A. Galarneau, M. Nader, F. Guenneau, F. D. Renzo, A. Gedeon, *J. Phys. Chem. C* **2007**, *111*, 8268.